Empirical mode decomposition to assess cardiovascular autonomic control in rats

Edmundo Pereira de Souza Neto[1,2,3],
Patrice Abry [1],
Patrick Loiseau[1],
Jean Christophe Cejka[2],
Marc Antoine Custaud[4],
Jean Frutoso[2],
Claude Gharib[2],
Patrick Flandrin[1].

(1) Laboratoire de Physique, CNRS UMR 5672, École Normale Supérieure de Lyon, 46, allée d'Italie, 69364 Lyon Cedex 07, France.
(2) Université Claude Bernard Lyon I, Laboratoire de Physiologie, Faculté de Médecine Lyon Grange-Blanche, 8 avenue Rockefeller, 69373 Lyon Cedex 08, France.
(3) Service d'Anesthésie Réanimation, Hôpital Cardio-Vasculaire et Pneumologique Louis Pradel, BP Lyon Monchat, 69394 Lyon Cedex 03, France,
et Equipe d'Accueil 1896, Université Claude Bernard Lyon 1,
8 avenue Rockefeller, 69373 Lyon Cedex 08, France.
(4) Laboratoire de Physiologie d'Angers, UMR CNRS 6188, Faculté de médecine d'Angers, 49033 Angers Cedex, France.

Short title : Empirical Mode Decomposition in Rats.

Corresponding author : Edmundo Pereira de Souza Neto
Laboratoire de Physique, CNRS UMR 5672,
École Normale Supérieure de Lyon,
46, allée d'Italie, 69364 Lyon Cedex 07, France
Tel.: (33) 47272 8493
Fax: (33) 47272 8950
E-mail: edmundo.pereira-de-souza@chu-lyon.fr

Abstract

Heart beat rate and blood pressure, together with baroreflex sensitivity, have become important tools in assessing cardiac autonomic system control and in studying sympathovagal balance. These analyses are usually performed thanks to spectral indices computed from standard spectral analysis techniques. However, standard spectral analysis and its corresponding rigid band pass filter formulation suffers from two major drawbacks. It can be significantly fooled by non stationarity issues and it proves unable to adjust to *natural* intra- and inter-individual variability. Empirical Mode Decomposition (EMD), a tool recently introduced in the literature, provides us with a signal adaptive decomposition that proves useful for the analysis of non-stationary data and shows a strong ability in precisely adjusting to the spectral content of the analyzed data. It is based on the concept that any complicated set of data can be decomposed into a finite number of components, called intrinsic mode functions, associated with different spectral contributions.

The goals of the present article are two folds. First, we study the changes in the sympathovagal balance induced by various pharmacological blockades (Phentolamine, Atropine and Atenolol) of the autonomic nervous system in normotensive rats. Second, we assess the use of Empirical Mode Decomposition for the analysis of the cardiac sympathovagal balance after pharmacological injections. To do so, we develop a new (EMD based) LF versus HF spectral decomposition of heart beat variability and systolic blood pressure, we define the corresponding EMD spectral indices and study their relevance to detect and analyze accurately changes in the sympathovagal balance without having recourse to any a priori fixed high-pass/low-pass filters.

Keywords : Autonomic Nervous System, RR Intervals, Blood Pressure, Alpha Gain, Rats, LF/HF decomposition, Empirical Mode Decomposition, Non Standard Spectral Analysis.

1 Motivation and Position of the Problem

Complex interactions exist between the sympathetic and parasympathetic systems, the two components of the autonomic nervous system. They act as a balance opposing neural mechanisms. Under selected stimulations, the dynamics of this balance mechanisms can be significantly altered [Ori et al., 1992]. Such modifications can be studied using relevant autonomic indices [Goldberger, 1999].

Heart rate variability (HRV) is a general term used to denote fluctuations in inter-beat intervals (i.e., intervals between consecutive heart beats or RR Intervals) and therefore in instantaneous heart rate. The analysis of heart rate variability has become increasingly important in physiological studies (cf. e.g., [Parati et al, 1995 , Stein and Kleiger, 1999]) and the support for using heart rate variability as an index for autonomic cardiovascular control comes from results demonstrating that heart rate variability is virtually abolished after parasympathetic and sympathetic blockades [Pagani et al., 1986].

Heart rate variability indices (such as the ratio between the powers of the low and high frequencies, or the normalized low frequency (LF) and high frequency (HF) powers) have been used to describe the sympathovagal balance [Malliani et al., 1991], [Ori et al., 1992], [Pagani et al., 1986]. Under normal circumstances, the HF power represents the vagal control of the heart, modulated by breathing, while the LF power (more precisely, its normalized version) reflects primarily the sympathetic modulation of heart rate [Malliani et al., 1991]. Finally, the LF/HF ratio characterizes the sympathovagal balance [Pagani et al., 1986], [Malliani et al., 1991]. However, other studies also suggest that the low frequency heart rate rhythms may have both sympathetic and vagal origins [Pomeranz et al., 1985], [Eckberg, 1997].

Although blood pressure is continuously modified by external stimulations, it spontaneously tends to

return to a stable point. When blood pressure decreases or rises, the baroreceptor activity decreases or increases accordingly, and influences heart rate, myocardial contractility, cardiac output, regional vasoactivity and blood flow distribution through its reflex action. Thus, baroreflex is important to counteract depressor or pressor stimuli and to cause arterial pressure to return to normal levels [Farah et al., 1999].

Quantitative analyses of the overall gain of baroreflex are commonly performed in terms of ratios of powers of the frequency contents of the RR Intervals and systolic blood pressure (SBP) variations. Hence, spectral analysis has become a standard method to study baroreflex and periodogram based estimates or autoregressive models are commonly used for the analysis of the corresponding data [Malliani et al., 1991 , Parati et al, 1995]. Such methods, which in most cases generate comparable results, are fundamentally relying on a stationarity of the data assumption and are linear in nature. However, there are situations where these assumptions are no longer valid. For instance, a sudden change can be imposed over the studied system or patient (see, e.g., [Souza Neto et al., 2002]). Also the spectral content of the data under study may spontaneously vary because it is naturally tied to a time-varying phenomenon (such as respiration). Moreover, baroreflex index definitions rely on the choice of an a priori and rigid low frequency - high frequency decomposition. Such an approach cannot account for the unavoidable intra- or inter-individual variability that naturally occurs. Therefore, to cope both with non-stationarity and natural variability issues, we propose to use a non standard spectral analysis based on a new approach, referred to as *Empirical Mode Decomposition* (EMD), recently developed by [Huang NE et al., 1998a] (See also [Huang and Shen, 2005]).

The aims of the present article are two folds. First, it is intended to assess the use of the *Empirical Mode Decomposition* to perform (non standard) spectral analysis so as to adaptively separate HF and LF components of RR Intervals and SBP and hence to analyze the baroreflex sensitivity. Second, it

is proposed to study the compared relevance and benefits of the use of EMD based autonomic indices versus standard ones for the characterization of the cardiac sympathovagal balance. This is achieved by performing adrenergic and cholinergic receptor blockades over a population of normotensive rats. Changes in the corresponding indices are studied after the pharmacological blockades of the autonomic nervous system.

2 Materials and Methods

2.1 Animals

After a 10-day lasting quarantine period, eight male Wistar rats (body weight 270 ± 20 g, IFFA-CREDO, Les Oncins, France) were used. They were housed in controlled conditions of temperature (22 ± 1 $^{\circ}$C), humidity (60 ± 10 %), and lighting (12-h light/dark cycle, 7:00 a.m. to 7:00 p.m. [light] and 7:00 p.m. to 7:00 a.m. [dark]). They were fed with standard rat chow containing 0.3 % sodium (Elevage UAR, Epinay sur Orge, France) and tap water ad libitum. The protocol is in accordance with the Guide for the Care and use of Laboratory Animals published by the US National Institutes of Health (NIH Publication No. 85-23, revised 1996).

2.2 Telemetry system

The telemetry system was purchased from Data Sciences International ^{TM} (St Paul, MN, USA). It is composed of an implantable transmitter Tl 11-M2-C50-PXT, a receiver RLA 1020, a pressure reference module C11 PR, a data acquisition system with a consolidation matrix BCM 100, for converting the radio-signal to electrical impulses, and a computer with a UA10 PC processor card for data recording and storing.

2.3 Surgical implantation

The rats were anesthetized with Halothane (2 % in oxygen). The telemetry transmitter was implanted 14 days before the study under aseptic conditions into the peritoneal cavity with the sensing catheter placed in the descending aorta below the renal arteries. Transmitter leads were sutured subcutaneously to the dorsal surface of the xiphoid process and into the anterior mediastinum close to the right atrium.

Body temperature was maintained at 38 ˚C using an electric heating pad during and after surgery until rats awakened. During the post-surgical period the animals were administered penicillin (15000 units s.c.) and buprenorphine (0.03 mg·kg^{-1} s.c.) for 3 days and monitored for general health and satisfactory blood pressure, pulse and heart rate.

Subsequently, 3 days before the study, rats were re-anesthetized with halothane (2 % in oxygen) and a polyethylene catheter (n° 2, i.d. 0.38 mm, e.d. 1.09 mm, Biotrol, Paris) was inserted into the lower inferior cava vein via the left femoral vein. The catheter was filled with heparinized Saline (50 U heparin/ml) and plugged with a short piece of stainless steel wire.

2.4 Experimental protocol

Four types of injections were performed:

- Saline 0.9 % (100 μl·kg^{-1} i.v; n = 8),
- Phentolamine (5 mg·kg^{-1} i.v., 10 mg·ml^{-1}, Sigma Chemical, St Louis, MO, USA; n=8),
- Atropine (0.5 mg·kg^{-1} i.v., 10 mg·ml^{-1}, Sigma; n=8),
- Atenolol (1 mg·kg^{-1} i.v., 10 mg·ml^{-1}, Sigma; n=8).

RR intervals and SBP will reflect the changes in the sympathovagal balance state induced by pharmacological blockades of the autonomic nervous system: a decrease of the parasympathetic effect after Atropine or a decrease of the sympathetic effect after Atenolol.

The rats were kept individually in a plexiglas cage placed above the receiver. Each rat was subjected to a total of four treatments with one injection per day (performed individually every other day). The order of treatments was randomized for each rat, hence a cumulative effect is improbable. Agonists were injected at the end of the recording to confirm adequate blockade. The beta 1-adrenergic blockade was demonstrated by the suppression of tachycardia to isoproterenol administration (0.2 μg·kg^{-1} i.v., Sigma). The efficacy of alpha 1-blockade by Phentolamine was assessed by the measurement of pressor responses to an intravenous injection of the alpha-adrenoceptor agonist phenylephrine (3 μg·kg^{-1} i.v., Sigma). Blood pressure and heart rate responses to metacholine (0.1 μg·kg^{-1} i.v., Sigma) were used to ensure the efficacy of cholinergic receptor blockade.

2.5 Data recording

RR Intervals and arterial blood pressure were monitored before and after injections. Data recording was performed only if the rats showed no sign of infection and had normal weight gain.

Recording sessions were always performed between 9:00 a.m. and 12:00 a.m. over a period of 15 min for each injection. Continuous data acquisition (ECG and blood pressure) at a sampling rate of 1000 Hz, was done on a PC Pentium ^{TM} 133 MHz with a 12-bit analogue-to-digital converter (AT-MIO-16E-10; National Instruments ^{TM}, Austin, TX, USA) equipped with a software developed with LabVIEW 4.0.1 software ^{TM} (National Instruments ^{TM}, Austin, TX, USA).

For each cardiac cycle, heart beat occurrence times, $\{t_i\}$, were extracted (from the ECG signal) and

the systolic and diastolic blood pressures were recorded at the corresponding times. Premature and post-extrasystolic beats were manually identified and edited by linear interpolation. Such beats represented < 2 % of all analyzed beats. The data analyzed in the present work therefore consist of the list of the RR intervals, $\{ R_i = t_{i+1} - t_i, i \in I\}$, together with the corresponding SBP, $\{P_i = \text{SBP}(t_i), i \in I\}$ and are hence irregularly sampled.

3 Data Analysis

3.1 Preprocessing

To transform the recorded data into a regularly sampled time series, the following preprocessing procedures are applied.

1. A sliding median filter is first applied to the RR Intervals and SBP series to replace outliers and/or abnormal values with a local average.
2. RR Intervals and SBP series are independently and regularly resampled with sampling frequency: $f_e = 10Hz$. It is chosen a priori high with respect to the *naturally* expected frequency content of the data. It is checked a posteriori that Shannon criterion is well-satisfied.
3. A standard linear detrending procedure is systematically applied independently on both time series.
4. Because they present significant very low frequency (VLF) components related to various phenomena (such as respiration, ...) that are not of interest for the present study, the data are high pass filtered. Based on results recalled below, the cut-off frequency is: $f_c = 0.25Hz$. This last operation is omitted when data are analyzed with EMD.

In the sequel, the data obtained from these operations will be denoted, with a little abuse of notation, $\{R_k = R(kT_e), k \in K\}$ and $\{P_k = P(kT_e), k \in K\}$, where $T_e = 1/f_e$. Examples of such time series are shown in Figs. 1 and 2, top rows.

3.2 Standard Spectral Analysis and Baroreflex Sensitivity

3.2.1 LH vs HF decomposition

The spectra, or power spectral densities (PSD), of the time series, as well as the cross-spectrum, are computed using a standard Periodogram spectral estimator (Hamming window). Estimated spectra were labeled S_R, S_P and S_{RP}, respectively. Examples are reported in Fig. 1 and Fig. 2, bottom rows.

Spectra are usually divided into three frequency bands appropriate to the cardiac frequency of the rat (cf. e.g., [Souza Neto et al., 2001]):

Very Low Frequency (VLF) : $f_{L_0} = 0.0195 \leq f \leq f_{H_0} = 0.26Hz$,

Low Frequency (LF) : $f_{L_1} = 0.26 \leq f \leq f_{H_1} = 0.75Hz$,

High Frequency (HF) : $f_{L_2} = 0.75 \leq f \leq f_{H_2} = 4.00Hz$.

The VLF oscillations are not studied. Absolute powers of each frequency band are computed by integrating PSD across the a priori chosen frequency bands:

$$\left.\begin{array}{llll} P_{R,LF} = \int_{f_{L_1}}^{f_{H_1}} S_R(f)df, & P_{R,HF} = \int_{f_{L_2}}^{f_{H_2}} S_R(f)df, \\ P_{P,LF} = \int_{f_{L_1}}^{f_{H_1}} S_P(f)df, & P_{P,HF} = \int_{f_{L_2}}^{f_{H_2}} S_P(f)df. \end{array}\right\} \quad (1)$$

The ratio LF/HF is defined as:

$$\text{LF/HF} = P_{R,LF}/P_{R,HF}. \quad (2)$$

Normalized powers enable us to perform comparisons between animals that are characterized by large variations in absolute PSDs. They are obtained by dividing the integrated PSDs within each frequency band (LF or HF) by the sum of the LF and HF absolute PSDs:

$$\left.\begin{array}{rcl} \tilde{P}_{R,LF} & = & P_{R,LF}/(P_{R,LF}+P_{R,HF}), \\ \tilde{P}_{R,HF} & = & P_{R,HF}/(P_{R,LF}+P_{R,HF}), \\ \tilde{P}_{P,LF} & = & P_{P,LF}/(P_{P,LF}+P_{P,HF}), \\ \tilde{P}_{P,HF} & = & P_{P,HF}/(P_{P,LF}+P_{P,HF}). \end{array}\right\} \quad (3)$$

3.2.2 Baroreflex sensitivity and Alpha Gains

The baro-sensitivity consists of the regulation mechanism that interrelates the fluctuations of RR Intervals to that of SBP. It can be characterized via two numbers referred to as the LF and HF Alpha Gains are defined as:

$$\alpha_{LF} = \int_{f_{L_1}}^{f_{H_1}} \gamma(f)\sqrt{\frac{S_R(f)}{S_P(f)}}df, \quad \alpha_{HF} = \int_{f_{L_2}}^{f_{H_2}} \gamma(f)\sqrt{\frac{S_R(f)}{S_P(f)}}df, \quad (4)$$

where the coherence function γ is defined as:

$$\gamma(f) = \frac{S_{RP}(f)}{\sqrt{S_R(f)S_P(f)}}. \quad (5)$$

3.3 Empirical Mode Decomposition and Baroreflex sensitivity

In a recent work, we proposed to define extensions of these Alpha Gains that allowed us to study the evolution along time of the baro-sensitivity and derived the corresponding algorithm (cf. [Custaud et al., 2002] for thorough details). However, in the present work, we mostly want to be able to account for natural intra- and inter-individual variabilities. To do so, we propose the use of a non standard spectral analysis based on the Empirical Mode Decomposition (EMD).

3.3.1 Empirical Mode Decomposition

The starting point of EMD is to consider oscillations at a very local level. In fact, when looking at the evolution of a signal $X(t)$ between two consecutive extrema (say, two minima m_- and m_+, occurring at times t_- and t_+, respectively). It becomes possible to heuristically define a (local) high-frequency part $d(t)$, or local detail, which corresponds to the oscillation terminating at the two minima and passing through the maximum M, that necessarily exists in between m_- and m_+. For the picture to be complete, one still has to identify the corresponding (local) low-frequency part $m(t)$, or local trend, so that we have $X(t) = m(t) + d(t)$ for $t_- < t < t_+$. Assuming this is done in some proper way for all the oscillations composing the entire signal, the procedure can then be applied on the residual consisting of all local trends. Constitutive components of a signal can therefore be iteratively extracted this way, the only definition of such a so-extracted "component," referred to as an *Intrinsic Mode Function* (IMF), being that it is locally (i.e., at the scale of one single oscillation) in the highest frequency band. Given a signal $X(t)$, the effective algorithm of EMD is as follows:

1. identify all extrema of $X(t)$
2. interpolate between minima (resp. maxima), ending up with some "envelope" $e_n(t)$ (resp. $e_M(t)$)
3. compute the average $m(t) = \frac{e_n(t)+e_M(t)}{2}$
4. extract the first "mode" as $d(t) = X(t) - m(t)$
5. iterate on the residual $m(t)$

In practice, the above procedure has to be refined by first iterating steps 1 to 4 upon the detail signal $d(t)$, until this latter can be considered as zero-mean according to some *stopping criterion*, this is usually referred to as the *sifting* procedure [Huang NE et al., 1998a]. The aims of this repeated operation is

to eliminate the riding waves and to achieve a more symmetrical wave-profile by smoothing the uneven amplitudes. It is suggested that a threshold is used, computed by summing the squared normalized differences from two consecutive sifting results, between 0.2 and 0.4 as a limit, to obtain the desired IMF first component [Huang NE et al., 1998a, Huang et al., 1998b, Huang et al., 1999, Echeverria et al., 2001]. Once this is achieved, the detail is considered as the effective IMF, the corresponding residual is computed and step 5 applies.

An IMF satisfies two conditions: in the whole data set, the number of extrema and the number of zero crossings must either equal or differ at most by one; and at any point, the mean value of the envelope defined by the local maxima and the envelope defined by the local minima is zero [Huang et al., 1999]. By construction, the number of extrema is decreased (on average, by a factor of 2) when going from one residual to the next. Modes and residuals are determined on spectral arguments, but it is worth stressing the fact that their high vs. low frequency discrimination applies only locally and corresponds by no way to a pre-determined sub-band filtering (as, e.g., in a wavelet transform). Selection of modes rather corresponds to an automatic and adaptive and hence signal-dependent (and possibly time-variant) filtering.

Given an input signal X to be analyzed, the output of the EMD procedure therefore consists of a set of IMFs whose number and contents are both signal and procedure parameter dependent. IMFs are numbered in increasing order $\mathrm{IMF}_{X,1}$, $\mathrm{IMF}_{X,2}$, ... from high frequency to low frequency contents.

3.3.2 Intrinsic Mode Function Association

Because IMFs are adaptively or self-chosen by the data under analysis, there is no reason why they should naturally match the *rigid* a priori VLF, LF, HF bandwidth division mentioned above. To be able

to perform an EMD based analysis of the Baroreflex sensitivity, we need to re-define EMD based LF and HF components. Based on observations detailed and made explicit in Section 4.2 below, we are able to define the HF and LF contributions of the RR Intervals and SBP time series by addition of well chosen IMFs (precise definitions are postponed to Section 4.2). They are labeled, R_{LF}, R_{HF}, P_{LF}, P_{HF} and $S_{R,LF}, S_{R,HF}, S_{P,LF}$ and $S_{P,HF}$ stand for their power spectra respectively. From those LF and HF components, the corresponding spectral indices can be defined (the $'$ are added to distinguish the EMD based quantities from the standard ones):

$$\left.\begin{array}{lcllcl} P'_{R,LF} & = & \int S_{R,LF}(f)df, & P'_{R,HF} & = & \int S_{R,HF}(f)df, \\ P'_{P,LF} & = & \int S_{P,LF}(f)df, & P'_{P,HF} & = & \int S_{P,HF}(f)df, \\ \text{(LF/HF)'} & = & P'_{R,LF}/P'_{R,HF}, & & & \\ \tilde{P}'_{R,LF} & = & P'_{R,LF}/(P'_{R,LF}+P'_{R,HF}), & \tilde{P}'_{R,HF} & = & P'_{R,HF}/(P'_{R,LF}+P'_{R,HF}), \\ \tilde{P}'_{P,LF} & = & P'_{P,LF}/(P'_{P,LF}+P'_{P,HF}), & \tilde{P}'_{P,HF} & = & P'_{P,HF}/(P'_{P,LF}+P'_{P,HF}). \end{array}\right\} \quad (6)$$

3.3.3 Baroreflex sensitivity: EMD based Alpha Gains

Because we no longer have two time series, R and P, but four, R_{HF}, R_{LF}, P_{HF}, P_{LF} to characterize the baroreflex sensitivity, we can no longer apply the Alpha Gains as defined in Eq. (4) above. We propose the following EMD extensions of these indices.

$$\left.\begin{array}{rcl} \alpha'_{LF} & = & \displaystyle\int_{\bar{f}_{P,LF}-\beta\Delta f_{P,LF}}^{\bar{f}_{P,LF}+\beta\Delta f_{P,LF}} \gamma_{LF}(f)\sqrt{\frac{S_{R,LF}(f)}{S_{P,LF}(f)}}df, \\ \alpha'_{HF} & = & \displaystyle\int_{\bar{f}_{P,HF}-\beta\Delta f_{P,HF}}^{\bar{f}_{P}+\beta\Delta f_{P,HF}} \gamma_{HF}(f)\sqrt{\frac{S_{R,HF}(f)}{S_{P,HF}(f)}}df. \end{array}\right\} \quad (7)$$

The central frequencies, $\bar{f}_{P,LF}, \bar{f}_{P,HF}$, the standard deviation spectral extensions, $\Delta f_{P,LF}, \Delta f_{P,HF}$ and the coherence functions, $\gamma'_{LF}, \gamma'_{HF}$, are defined as:

$$\left.\begin{array}{rcl} \bar{f}_{P,LF} & = & \displaystyle\int f.S_{P,LF}(f)df / \int S_{P,LF}(f)df, \\ \Delta f_{P,LF} & = & \displaystyle\left(\int (f-\bar{f}_{P,LF})^2 S_{P,LF}(f)df / \int S_{P,LF}(f)df\right)^{1/2}, \\ \gamma'_{LF}(f) & = & \frac{S_{RP,LF}(f)}{\sqrt{S_{R,LF}(f)S_{P,LF}(f)}}. \end{array}\right\} \quad (8)$$

For HF quantities, the corresponding definitions hold changing LH into HF.

The definition of α'_{LF} (resp., of α'_{HF}) involves a division by P_{LF} (resp., P_{HF}). By construction, P_{LF} (resp., P_{HF}) is a band pass process and it is experimentally observed that its spectrum mostly vanishes outside the range $\bar{f}_{P,LF} - 2\Delta f_{P,LF} \leq f \leq \bar{f}_{P,LF} + 2\Delta f_{P,LF}$ (resp., $\bar{f}_{P,HF} - 2\Delta f_{P,HF} \leq f \leq \bar{f}_{P,HF} + 2\Delta f_{P,HF}$) (cf. Figs 7 and 8). This leads us to restrict accordingly the integration range, making use of the tunable parameter $\beta > 0$ whose precise choice will be further discussed (cf. Section 4.3). Obviously, R_{HF} and R_{LF} also consist of band pass processes. Because they are involved in the numerator of the EMD-gain definitions, they do not imply any restriction. Moreover, for most cases, it can be observed that $f_{P,LF}, \Delta f_{P,LF}$ and $f_{R,LF}, \Delta f_{R,LF}$ closely coincide (resp., $f_{P,HF}, \Delta f_{P,HF}$ and $f_{R,HF}, \Delta f_{R,HF}$).

3.4 Statistical tests and significant changes

Non-parametric Friedman test associated with the Wilcoxon matched pairs test corrected for multiple comparisons were performed for comparisons between base, Saline, $\alpha 1 - \beta 1-$ and cholinergic blockades. Wilcoxon's test for paired data was used to study agonist effects before and after blockade. Statistical analysis was performed using the StatView TM software for Windows (1996, version 4.57, Abacus Concepts Inc., Berkeley, CA, USA). Results are reported in tables (cf. Tables 1 to 4) and are expressed in terms of median $\pm$ median absolute deviation. The usual $p \leq 5\,\%$ significance level is used and significant changes are marked with stars in tables.

3.5 Analysis Routines

The EMD procedures and the corresponding non standard spectral analysis as well as the standard one and the change test were developed by ourselves in Matlab, Mathworks^{TM}, using the signal processing

and statistical toolboxes, together with the Time-Frequency toolbox [Auger et al., 1995]. The EMD codes are available at perso.ens-lyon.fr/patrick.flandrin.

4 EMD procedure: practical issues, HF/LF decomposition and Alpha Gains

Prior to describing the results obtained on the sympatovagal balance analysis (cf. Section 5), this section aims at detailing practical issues in the implementation of the EMD procedure as well as the experimental results leading to the definition of the rules for the IMF association and hence to the EMD LF and HF decomposition.

4.1 Practical difficulties in implementation

• **Sampling Rate.** It has been observed empirically that the EMD procedure presents a better stability with respect to the frequency contents of the obtained IMFs when the analyzed data are sufficiently oversampled. It can be seen (cf. Figs 1 and 2) that the frequency contents of the data essentially vanish above 3Hz. It has been chosen to sample the data at 10Hz so that not only Shannon sampling theorem is respected but the data are significantly oversampled. Higher oversampling frequencies do not improve the obtained results but may induce significantly higher computational costs.

• **Sifting iteration number.** As described in Section 3.3 above, a key element in the construction of the IMF lies in the choice of a stopping criterion qualifying how close it is from a zero-mean component and hence controlling the maximum number of allowed sifting iterations. Experimentally, we observed that allowing a too large number of iterations is not a desirable fact. It means first a high computational

cost. Second and foremost, it results in the creation of *artificial* frequency contents in IMFs. Indeed, to satisfy a severe stopping criterion, the EMD procedure tends to produce energy in the very low and low frequency ranges for the first IMF. Because EMD ensures perfect reconstruction by linear addition of IMFs, this, in turns, also create artificial energy in the same frequency ranges for the subsequent IMFs, hence a propagation of the defect across IMFs. A careful examination of the IMFs computed for each subject led us to choose to stop the sifting procedure either when a non severe criterion is satisfied or when a maximum number of iterations is reached. Practical experimentations led us to choose this maximum to 20. We carefully checked that the results reported in the present work do not depend on this precise choice of the iteration number and remain consistent when this number is varied from 15 to 100.

4.2 IMF Frequency contents and EMD based LF and HF decomposition

• **IMF Frequency contents.** Figs. 3 and 4 present the superimposition of the spectra for IMF 1 to 6 obtained from all analyzed RR Intervals and SBP time series respectively. For RR Intervals, Fig. 3 shows that the spectral contents of the four first IMFs fall within the HF and LF frequency bands, while all the subsequent IMFs are in the VLF frequency band or even below. This is why only the four first IMFs are considered for the RR Intervals time series. The same holds for the three first IMFs of the SBP time series. As an example, the periodogram based estimates of the spectra of the five first IMFs for RR Intervals and SBP of two given rats are shown in Fig. 5 and Fig. 6. For each IMF, the rigid position of the VLF, LF, HF bandwidth division are reported in black dashed vertical lines. The central frequency and the standard deviation spectral extension, that summarize the frequency content of the IMFs, are also represented with red crosses. They are defined as in Eqs. (8), mutatis mutandis.

Together, the examination of these four figures enable us to draw two major conclusions. First, in all cases IMFs with labels strictly larger than 4 correspond to VLF or even lower frequencies. They will not be further studied. Second, for RR Intervals time series, IMF1 and IMF2 have spectral contents that are systematically mainly spread within the HF band, while those of IMF3 and IMF4 fall in the LF band. For SBP time series, the spectrum of IMF1 corresponds to HF and whose of IMF2 and IMF3 to LF. These considerations led us to propose the following EMD-driven definitions of the HF and LF contributions of the RR Intervals and SBP time series (cf. Section 3.3 above):

$$\left.\begin{array}{rcl} R_{HF}(t) & = & \text{IMF}_{R,1}(t) + \text{IMF}_{R,2}(t), \\ R_{LF}(t) & = & \text{IMF}_{R,3}(t) + \text{IMF}_{R,4}(t), \\ P_{HF}(t) & = & \text{IMF}_{P,1}(t), \\ P_{LF}(t) & = & \text{IMF}_{P,2}(t) + \text{IMF}_{P,3}(t). \end{array}\right\} \tag{9}$$

We checked manually rat by rat and injection by injection that these associations are meaningful for each case.

• **EMD based LF and HF decomposition.** Figs. 7 and 8 give examples of the spectral contents of R_{HF}, R_{LF}, P_{HF}, P_{LF} for two different subjects, chosen as representative for the two characteristic situations practically observed: the EMD LF/HF decomposition matches the a priori rigid bands (Example 1) or it does not (Example 2). On the plots, the a priori LF/HF separations are shown with black dashed vertical lines, while the central frequency and the standard deviation spectral extension are pictured in solid line (red) crosses. Their definitions are adapted straightforwardly from Eqs. (8). Fig. 7 is representative for a large number of rats and injections, one sees that the frequency ranges of the EMD LF and HF contributions (R_{LF} and R_{LF}, P_{HF} and P_{HF}, resp.) spontaneously match those of the a priori rigid LF and HF bands. This is not an input of the approach and hence constitute per se a first interesting result validating the use of EMD: when the frequency contents of the data naturally matches the a priori rigid LF and HF bands, EMD provides us with this decomposition.

Fig. 8 shows the spectral contents of the LF and HF EMD components for another subject. For this particular individual, it can be noticed that, for both RR Intervals and SBP, the LF components are significantly shifted towards lower frequencies. A large portion of the corresponding energy would have been considered VLF with the classical approach and not taken into account into the study of the sympathovagal balance while it is actually included in this balance determination with the EMD approach. This second example is chosen as a representative of a second group of (numerous) individuals, for which the EMD based LF and HF components do not exactly match the rigid a priori frequency band decomposition.

In the former example, standard and non standard spectral analysis yield equivalent values for the computed indices, while in the latter, significant differences are observed. Our interpretation of these discrepancies is the following: The spectral content of the data that can be associated to the sympathetic and parasympathetic activities do not naturally fall *exactly* within the a priori chosen rigid frequency bands. Because of inter- and intra- individual natural or external variabilities, this bands may be slightly shifted from one measurement to the other (see e.g., [Novak and Novak, 1993, Ramaekers et al., 2002]) and EMD spontaneously accounts for these natural variations. The key point of our approach therefore lies in the fact that we obtain a LF versus HF separation without resorting to a priori chosen and rigid band pass filters. The a priori LF/HF separation defined above is now only used a guide line to decide whether IMFs belong to LF or HF. This is the improvements brought by the use of EMD.

4.3 EMD Alpha Gains: Choosing the β parameter

The parameter β in Eq. (7)) is related to the extension in the frequency domain of the spectra of the band-pass processes P_{LF} and P_{HF}. The choice of its value results from a trade-off that can be formulated as

follows: a too large β would yield an overlap in the integration frequency bands and is hence against the intuition of a LF vs HF decomposition. A too small β would result in highly fluctuating non robust EMD Alpha Gains. Again, a careful examination of this issue led us to choose $\beta = 1$ (as represented in the figures). We checked that the results reported here do not significantly depend on the precise choice of β in a range $0.5 \leq \beta \leq 1.2$. Moreover, the ranges $\overline{f}_{P,LF} - \Delta f_{P,LF} \leq f \leq \overline{f}_{P,LF} + \Delta f_{p,LF}$ and $\overline{f}_{p,HF} - \Delta f_{p,HF} \leq f \leq \overline{f}_{p,HF} + \Delta f_{P,HF}$ tend to spontaneously match the a priori chosen widths of the LF and HF bands. This is not an a priori input of the method and can be considered as a significant a posteriori validation of the choice $\beta = 1$.

5 Experimental results

5.1 Time domain analysis

Injections did not induce stress in animals and no sign of restlessness or irritation appeared. After Phentolamine, Phenylephrine did not change systolic blood pressure (Δ = 5 $\pm$ 3 mmHg). Metacholine did not change RR intervals (Δ = 10 $\pm$ 7 ms) or systolic blood pressure (Δ = -6 $\pm$ 3 mmHg) after Atropine. Isoproterenol induced no significant change in RR intervals after Atenolol (Δ = 10 $\pm$ 8 ms).

Time domain measures of RR intervals systolic and diastolic blood pressure are reported in Table 1. Saline injections do not induce any significant change in the global time domain indices. All other injections do. Phentolamine reduced RR intervals by 30 %, systolic and diastolic blood pressure by 26 % and 17 % respectively. Atropine reduced RR intervals by 24 %, and increased systolic and diastolic blood pressure by 11 % and 16 % respectively. Atenolol increased RR intervals by 11 % and reduced systolic and diastolic blood pressure by 9 %.

5.2 Standard spectral analysis

Tables 2 and 3 (top parts) summarize the values of various indices computed on RR Intervals and SBP, respectively, using the standard spectral analysis and change detection test described above.

For RR Intervals, Atropine reduces LF (58 %), HF (84 %), normalized HF (19 %) and increases LF/HF ratio (56 %) and normalized LF (28 %).

For SBP, Atropine induces a significant increase in LF (234 %), HF (94 %) and normalized LF (118 %) and reduces normalized HF (34 %).

Table 4 (top part) reports the changes in the Alpha Gains. Baroreflex sensitivity, measured by the LF and HF Alpha Gain indices, decreases after Atropine (62 %, 79 % respectively).

5.3 EMD based spectral analysis

Tables 2, 3 and 4 (bottom parts) gather the values taken by the EMD based spectral indices for RR Intervals and SBP as well as Alpha Gains.

For RR Intervals, Phentolamine increases the normalized HF (42 %) while Reducing normalized LF (28 %) and LF/HF (49 %). Atropine reduced HF (76 %) and normalized HF (39 %) and increased normalized LF (26 %) and LF/HF (107 %). Atenolol induced significant increase in normalized HF (48 %) and reduced normalized LF (33 %) and LF/HF (55 %).

For SBP, Atropine reduces the normalized HF (52 %) and increases the LF (253 %), HF (50 %) and normalized LF (15 %).

For the baroreflex sensitivity, α'_{LF} is decreased after Atropine and Atenolol (72 %, 50 % respectively) while α'_{HF} is decreased after Atropine (69 %).

6 Discussion

The combined use of a priori chosen and rigid frequency bands (and of the corresponding band pass filters) together with standard (parametric or non parametric) spectral techniques, leading to the definitions of Alpha Gains as in Eq. (4), suffers from two major limitations [Huang et al., 1998b]: First, they rely on a perfect stationarity assumption for the analyzed data. Second, they assume that the frequency band definitions used above in the low vs high frequency decompositions are absolute and cannot depend on the data. The *Empirical Mode Decomposition* (EMD) based spectral analysis approach provides the user with a valuable tool to overcome those two difficulties (cf. [Huang NE et al., 1998a, Huang et al., 1998b, Huang et al., 1999]).

In the present study, we mostly analyze subjects under stable conditions (after injections, a delay is respected before data recording) so that the data remain reasonably stationary within the analysis time window. However, potential developments under investigations consist in studying transient states such as those observed during or just after injections. For such situations, producing highly non stationary time series, we proposed, in a recent work, to define an extension of these gains that allowed us to study the evolution along time of the baro-sensitivity and derived the corresponding algorithm (cf. [Custaud et al., 2002] for thorough details). However, EMD also proves helpful. This is under investigation. For the work reported in the present contribution, the baro-sensitivity of the rats presents a strong and significant inter-subject variability. For instance, the frequency band decomposition corresponding to the sympathovagal balance may indeed slightly vary from one rat to the other according to its age, gender,... Also, it is well-known that the baro-sensitivity of a given subject is likely to be spontaneously and dynamically modified or (slightly) shifted under an imposed change or external circumstances (such

as stress, fatigue, respiration rate ...). To account for and accommodate both these *inter* and *intra* individual variations, we have chosen to use the *Empirical Mode Decomposition*, because of its being a highly signal adaptive frequency decomposition.

Let us now compare the results obtained from standard and EMD based spectral indices.

For RR Intervals, most of the significant changes detected by standard spectral analysis are also seen by EMD. For SBP, standard spectral analysis and EMD are in perfect agreement. These results can be read as a clear validation of the fact that the EMD based spectral analysis proposed in the present work provides us with a meaningful spectral analysis tool.

One can further notice that for RR Intervals a number of significant changes are detected by EMD when they are missed by standard spectral analysis (cf. Table 2). Let us carefully analyze these cases. A close inspection shows that for Atenolol, detections are missed by standard spectral analysis because the p-values (not reported here for sake of clarity of the Tables, but available upon request) are slightly above but very close to the $5\,\%$ threshold value that yields a detection. Hence, we can argue that the EMD approach better takes into account the inter-individual variability and hence better achieves the LF and HF decomposition and the corresponding sympatovagal analysis. Therefore, it enables us to clearly detect changes that are significant and are only *slightly* missed by standard spectral analysis because of its rigid a priori choices.

For Phentolamine, the situation is very different. Changes detected by EMD are totally missed by standard spectral analysis (the corresponding p-values are large). The reduction of the RR Intervals normalized LF component after Phentolamine, an alpha 1-adrenoreceptor blocker, suggests a strong link between the RR Intervals low frequency oscillations and the sympathetic vasomotor activity. This

confirms results in [Malliani et al., 1991], [Pagani et al., 1986], [Rubini et al., 1993]. Also, it has been reported in [Akselrod et al., 1987], [Herijgers & Flameng, 1998] that Phentolamine administration withdraws the vasomotor tone which is mainly sympathetic in rats.

Moreover, it is interesting that an increase in the RR Intervals normalized HF component is observed after Phentolamine injection (cf. Table 2). In addition to its well-known ability to block alpha 1-adrenoreceptors on vascular smooth muscles, Phentolamine also has a central sympathetic withdrawal action (cf. [Herijgers & Flameng, 1998], [Hilliard et al., 1972]) hence yielding an RR Intervals normalized HF increase.

Therefore, in comparison to standard spectral analysis that misses sympathovagal balance alterations after Phentolamine administration, EMD hence shows a better ability to detect them.

Let us now turn to baroreflex sensitivity. Low frequency baroreflex sensitivity decreases after Atropine and Atenolol. However, it is reduced less by beta-blockade than it is by administration of Atropine, indicating the predominance of vagal effects in this measure of the baroreflex sensitivity (Ramaekers et al., 2002). Therefore, it is worth noting here that the EMD based low frequency Alpha Gain index detects changes both for Atropine and Atenolol while the standard spectral analysis one is blind to the latter (cf. Table 4).

For High frequency baroreflex sensitivity, both tools detect the change induced by Atropine. For Phentolamine, the standard index sees a change when the EMD based one does not (cf. Table 4). This may be explained by the effect of respiration on RR Intervals, known as the respiratory sinus arrhythmia. Without standardization against the respiratory rate (which we did not measure in our study), high frequency changes cannot be fully and relevantly studied [Saul et al., 1989], [Perlini et al., 1995]).

Therefore, in all situations where discrepancies between the results obtained with EMD and standard spectral analysis were observed, a number of arguments can be proposed that indicate that EMD provides us with a finer analysis of the sympathovagal balance modifications.

7 Conclusion and perspectives

In the present work, we have assessed the relevance of various spectral indices for the detection and analysis of changes in the sympatovagal balance. We have shown that the use of a non standard spectral analysis based on Empirical Mode Decomposition brings improvements compared to standard spectral analysis. This is mainly because it enables to account for the natural intra- and inter-individual variabilities. Indeed, it avoids the drawbacks induced by the choice of priori, rigid, and uniform, for all individuals, band-pass filters. Also, we showed that the use of EMD requires significant attention regarding implementation issues such as sampling rate, sifting procedure stopping criterion, IMF association procedure and Alpha Gain definitions. The EMD based spectral analysis requires further developments under investigations to be made fully automatic.

Because EMD is naturally designed to address non stationarities, the non standard spectral analysis developed here could be fruitfully extended to situations where a dynamical change is imposed to the patient and where the study of the dynamical behavior of the baroreflex sensitivity is of interest. This EMD approach can also relevantly be compared to other ones based on time-frequency representations [Cohen, 1995], [Novak and Novak, 1993], [Flandrin, 1999] that provide indications regarding the way the spectral energy distribution of a signal varies along time. Also, we believe that the potentialities of the EMD based approach developed here are such that it could be successfully used in other

physiological situations to provide new observations more directly applicable to research in physiology [Gustin et al., 1998]. Further studies are necessary in animals and in humans to assess the use of this method to study alterations induced by hypertension, diabetes or other transition periods like arrhythmia.

8 Acknowledgements

This work was supported by grants from the Centre National d'Etudes Spatiales (CNES) and Groupement d'Intérêt Public (GIP) Exercice.

The authors gratefully acknowledge Gabriel Rilling, PhD student at ENS Lyon, who helped them in adapting and in modifying the EMD routines.

References

[Akselrod et al., 1987] Akselrod, S., Eliash, S., Oz, O., Cohen, S., 1987. Hemodynamic regulation in SHR: investigation by spectral analysis. Am. J. Physiol. 253, H176-H183

[Auger et al., 1995] Auger, F., Flandrin, P., Gonçalvès, P., Lemoine, O. Time-frequency toolbox for Matlab. Freeware at URL (http://tftb.nongnu.org)

[Cohen, 1995] Cohen, L., 1995. Time-Frequency Analysis. Prentice-Hall.

[Custaud et al., 2002] Custaud, M.A., de Souza Neto, E.P., Abry, P., Flandrin, P., Millet, C., Duvareille, M., Fortrat, J.O., Gharib, C., 2002. Orthostatic tolerance and spontaneous baroreflex sensitivity in men versus women after 7 days of head-down bed rest. Auton. Neurosci., 100, 66-76

[Echeverria et al., 2001] Echeverria, J.C., Crowe, J.A., Woolfson, M.S., Hayes-Gill, B.R., 2001. Application of empirical mode decomposition to heart rate variability analysis. Med. Biol. Eng. Comput., 39, 471-479

[Eckberg, 1997] Eckberg, D.L., 1997. Sympathovagal balance: a critical appraisal. Circulation, 96, 3224-3232

[Farah et al., 1999] Farah, V.M.A., Moreira, E.D., Pires, M.D., Irigoyen, M.C.C., Krieger, E.M., , 1999. Comparison of three methods for the determination of baroreflex sensitivity in conscious rats. Braz. J. Med. Biol. Res., 32, 361-369

[Flandrin, 1999] Flandrin, P., 1999. Time-Frequency/Time-Scale Analysis. Academic Press.

[Gustin et al., 1998] M.-P. Gustin, C. Cerutti, R. Unterreiner and C. Paultre, 1998. Identification of spontaneous cardiac baroreflex episodes at different timescales in rats. Am. J. Physiol., 274, H488-H493

[Goldberger, 1999] Goldberger, J.J., 1999. Sympathovagal balance: how should we measure it? Am. J. Physiol., 45, H1273-H1280

[Herijgers & Flameng, 1998] Herijgers, P., Flameng, W., 1998. The effect of brain death on cardiovascular function in rats. Part II. The cause of the in vivo haemodynamic changes. Cardiovasc. Res., 38, 107-115

[Hilliard et al., 1972] Hilliard, C.C., Bagwell, E.E., Daniell H.B., 1972. Effects of sympathetic and central nervous system alterations on the blood pressure responses to Phentolamine. J. Pharmacol. Exp. Ther., 180, 743-747

[Huang NE et al., 1998a] Huang, N.E., Shen, Z., Long, S.R., Wu, M.L.C., Shih, H.H., Zheng, Q.N., Yen, N.C., Tung, C.C., Liu, H.H., 1998. The empirical mode decomposition and the Hilbert spectrum for nonlinear and non-stationary time series analysis. Proc. R. Soc. Lond. A, 454, 903-995

[Huang et al., 1998b] Huang, W., Shen, Z., Huang, N.E., Fung, Y.C., 1998. Use of intrinsic modes in biology: examples of indicial response of pulmonary blood pressure to +/- step hypoxia. Proc. Natl. Acad. Sci. U.S.A., 95, 12766-12771

[Huang et al., 1999] Huang, W., Shen, Z., Huang, N.E., Fung, Y.C., 1999. Nonlinear indicial response of complex nonstationary oscillations as pulmonary hypertension responding to step hypoxia. Proc. Natl. Acad. Sci. U.S.A., 96, 1834-1839

[Huang and Shen, 2005] Huang, N.E., Shen, S.S.P., eds., 2005. Hilbert-Huang Transform and its Applications. World Scientific.

[Malliani et al., 1991] Malliani, A., Pagani, M., Lombardi, F., Cerutti, S., 1991. Cardiovascular neural regulation explored in the frequency domain. Circulation, 84, 482-492

[Novak and Novak, 1993] Novak, P., Novak, V., 1993. Time/frequency mapping of the heart rate, blood pressure and respiratory signals. Med. Biol. Eng. Comput., 31, 103-110

[Ori et al., 1992] Ori, Z., Monir, G., Weiss, J., Sahyouni, X.N., and Singer, D.H., 1992. Heart rate variability: frequency domain analysis. Cardiol. Clin., 10, 499-538

[Pagani et al., 1986] Pagani, M., Lombardi, F., Guzzetti, S., Rimoldi O., Furlan, R., Pizzinelli, P., Sandrone, G., Malfatto, G., Dell'Orto, S., Piccaluga, E., Turiel, M., Baselli, G., Cerutti, S., Malliani, A., 1986. Power spectral analysis of heart rate and arterial pressure variabilities as a marker of sympatho-vagal interaction in man and conscious dog. Circ. Res., 59, 179-193

[Parati et al, 1995] Parati G., Saul J.P., Di Rienzo M., Mancia G., 1995. Spectral analysis of blood pressure and heart rate variability in evaluating cardiovascular regulation-A critical appraisal. Hypertension, 25, 1276-1286

[Perlini et al., 1995] Perlini, S., Giangregorio, F., Coco, M., Radaelli, A., Solda, P.L., Bernardi, L., Ferrari, A.U., 1995. Autonomic and ventilatory components of heart rate and blood pressure variability in freely behaving rats. Am. J. Physiol., 269, H1729-H1734

[Pomeranz et al., 1985] Pomeranz, B., MaCaulay, R.J.B., Caudill, M.A., Kutz, I., Adam, D., Gordon, D., Kilborn, K.M., Barger, A.C., Shannon, D.C., Cohen, R.J., and Benson, H., 1985. Assessment of autonomic function in humans by heart rate spectral analysis. Am. J. Physiol., 248, H151-H153

[Ramaekers et al., 2002] Ramaekers, D., Beckers, F., Demeulemeester, H., Aubert, A.E., 2002. Cardiovascular autonomic function in conscious rats: a novel approach to facilitate stationary conditions. Ann. Noninvasive Electrocardiol., 7, 307-318

[Rubini et al., 1993] Rubini, R., Porta, A., Baselli, G., Cerutti, S., Paro, M., 1993. Power spectrum analysis of cardiovascular variability monitored by telemetry in conscious unrestrained rats. J. Auton. Nerv. Syst., 45, 181-190

[Saul et al., 1989] Saul, J.P., Berger, R.D., Chen, M.H., Cohen, R.J., 1989. Transfer function analysis of autonomic regulation. II. Respiratory sinus arrhythmia. Am. J. Physiol., 256, H153-H161

[Souza Neto et al., 2001] Souza Neto, E.P., Custaud., M.A, Frutoso, J., Somody, L., Gharib, C., Fortrat J.O., 2001. Smoothed pseudo Wigner-Ville distribution as an alternative to Fourier transform in rats. Auton. Neurosci., 87, 258-267.

[Souza Neto et al., 2002] Souza Neto, E.P., Custaud, M.A, Cejka, J.C., Abry, P., Frutoso, J., Gharib, C., Flandrin, P., 2002. Assessment of cardiovascular autonomic control by the empirical mode decomposition. Proceedings IV International Workshop Biosignal Interpretation BSI2002, pp. 123-126, Como, Italy.

[Stein and Kleiger, 1999] Stein, P.K., Kleiger, R.E., 1999. Insights from the study of heart rate variability. Annu. Rev. Med., 50, 249-261

	Control	**Saline** $(0.9\ \%)$	**Phentolamine** $(10\ \mathrm{mg}\cdot\mathrm{ml}^{-1})$	**Atropine** $(10\ \mathrm{mg}\cdot\mathrm{ml}^{-1})$	**Atenolol** $(10\ \mathrm{mg}\cdot\mathrm{ml}^{-1})$
RR intervals $(\mathbf{ms})$	170 ± 3	172 ± 5	$122 \pm 4^*$	$128 \pm 5^*$	$188 \pm 3^*$
SBP $(\mathbf{mmHg})$	121 ± 5	125 ± 7	$95 \pm 7^*$	$135 \pm 6^*$	$110 \pm 8^*$
DBP $(\mathbf{mmHg})$	92 ± 3	90 ± 5	$76 \pm 3^*$	$107 \pm 2^*$	$80 \pm 3^*$

Table 1: Time domain measures of RR intervals, systolic **SBP** and diastolic **DBP** blood pressures in different experimental conditions for 8 conscious rats. Results are expressed in terms of median $\pm$ median absolute deviation and the stars, *, indicate a significant change compared to the control value (as detected using a non parametric Friedman test, cf. Section 3.4).

		Control	**Saline** $(0.9\ \%)$	**Phentolamine** $(10\ \mathrm{mg}\cdot\mathrm{ml}^{-1})$	**Atropine** $(10\ \mathrm{mg}\cdot\mathrm{ml}^{-1})$	**Atenolol** $(10\ \mathrm{mg}\cdot\mathrm{ml}^{-1})$
$Standard$	$P_{R,LF}$	0.36 ± 0.16	0.43 ± 0.23	0.14 ± 0.67	$0.15 \pm 0.13^*$	0.43 ± 0.43
	$P_{R,LF}$	0.56 ± 0.22	0.62 ± 0.24	0.26 ± 0.94	$0.10 \pm 0.10^*$	0.92 ± 1.10
	$\tilde{P}_{R,LF}$	0.41 ± 0.03	0.40 ± 0.04	0.37 ± 0.07	$0.52 \pm 0.10^*$	0.31 ± 0.10
	$\tilde{P}_{R,HF}$	0.59 ± 0.03	0.60 ± 0.04	0.63 ± 0.07	$0.48 \pm 0.10^*$	0.69 ± 0.10
	LF/HF	0.68 ± 0.08	0.672 ± 0.12	0.581 ± 0.17	$1.06 \pm 0.55^*$	0.45 ± 0.21
EMD	$P'_{R,LF}$	1.00 ± 0.35	0.90 ± 0.47	0.28 ± 1.60	0.96 ± 0.87	0.90 ± 0.78
	$P'_{R,HF}$	0.74 ± 0.31	0.83 ± 0.32	0.36 ± 1.40	$0.18 \pm 0.23^*$	1.30 ± 1.60
	$\tilde{P}'_{R,LF}$	0.60 ± 0.06	0.57 ± 0.05	$0.43 \pm 0.07^*$	$0.75 \pm 0.11^*$	$0.40 \pm 0.12^*$
	$\tilde{P}'_{R,HF}$	0.40 ± 0.06	0.43 ± 0.05	$0.57 \pm 0.07^*$	$0.25 \pm 0.11^*$	$0.60 \pm 0.12^*$
	LF/HF	1.48 ± 0.30	1.35 ± 0.22	$0.75 \pm 0.23^*$	$3.10 \pm 2.40^*$	$0.67 \pm 0.36^*$

Table 2: **Standard vs EMD based Spectral Analysis Indices: RR Intervals.** LF and HF, absolute and normalized powers, and LF/HF ratio, top part: computed from standard spectral analysis (cf. Section 3.2), bottom part: computed from EMD (cf. Section 3.3). Powers are expressed in $10^3 ms^2/Hz$. Results are expressed as in Table 1.

		Control	**Saline** ($0.9\ \%$)	**Phentolamine** ($10\ \mathrm{mg}\cdot\mathrm{ml}^{-1}$)	**Atropine** ($10\ \mathrm{mg}\cdot\mathrm{ml}^{-1}$)	**Atenolol** ($10\ \mathrm{mg}\cdot\mathrm{ml}^{-1}$)
$Standard$	$P_{P,LF}$	0.29 ± 0.16	0.32 ± 0.16	0.28 ± 0.31	$0.97 \pm 0.23^{*}$	0.24 ± 0.17
	$P_{P,HF}$	0.16 ± 0.08	0.18 ± 0.10	0.33 ± 0.17	$0.31 \pm 0.07^{*}$	0.15 ± 0.15
	$\tilde{P}_{P,LF}$	0.64 ± 0.06	0.70 ± 0.05	0.51 ± 0.16	$0.77 \pm 0.03^{*}$	0.64 ± 0.11
	$\tilde{P}_{P,HF}$	0.36 ± 0.06	0.30 ± 0.05	0.49 ± 0.16	$0.23 \pm 0.03^{*}$	0.36 ± 0.11
EMD	$P'_{P,LF}$	0.51 ± 0.30	0.52 ± 0.26	0.42 ± 0.42	$1.80 \pm 0.52^{*}$	0.35 ± 0.34
	$P'_{P,HF}$	0.14 ± 0.08	0.17 ± 0.09	0.24 ± 0.14	$0.20 \pm 0.05^{*}$	0.14 ± 0.14
	$\tilde{P}'_{P,LF}$	0.78 ± 0.06	0.79 ± 0.03	0.64 ± 0.16	$0.89 \pm 0.03^{*}$	0.77 ± 0.10
	$\tilde{P}'_{P,HF}$	0.22 ± 0.06	0.23 ± 0.03	0.37 ± 0.16	$0.11 \pm 0.03^{*}$	0.23 ± 0.10

Table 3: **Standard vs EMD based Spectral Analysis Indices: Systolic blood pressure.** LF and HF, absolute and normalized powers, top part: computed from standard spectral analysis (cf. Section 3.2), bottom part: computed from EMD (cf. Section 3.3). Powers are expressed in $10^3 mmHg^2/Hz$. Results are expressed as in Table 1.

		Control	**Saline** ($0.9\ \%$)	**Phentolamine** ($10\ \mathrm{mg}\cdot\mathrm{ml}^{-1}$)	**Atropine** ($10\ \mathrm{mg}\cdot\mathrm{ml}^{-1}$)	**Atenolol** ($10\ \mathrm{mg}\cdot\mathrm{ml}^{-1}$)
$Standard$	α_{LF}	0.07 ± 0.13	0.13 ± 0.13	0.07 ± 0.03	$0.03 \pm 0.01^{*}$	0.06 ± 0.05
	α_{HF}	0.56 ± 0.49	0.59 ± 0.50	$0.22 \pm 0.22^{*}$	$0.12 \pm 0.02^{*}$	0.34 ± 1.00
EMD	α'_{LF}	0.10 ± 0.12	0.14 ± 0.12	0.08 ± 0.08	$0.03 \pm 0.04^{*}$	$0.05 \pm 0.03^{*}$
	α'_{HF}	0.68 ± 0.50	0.37 ± 0.40	0.16 ± 0.67	$0.21 \pm 0.06^{*}$	0.39 ± 1.2

Table 4: **Standard vs EMD Alpha Gains.** LF and HF Alpha Gains, top part: computed from standard spectral analysis (cf. Section 3.2), bottom part: computed from EMD (cf. Section 3.3). Results are expressed as in Table 1.

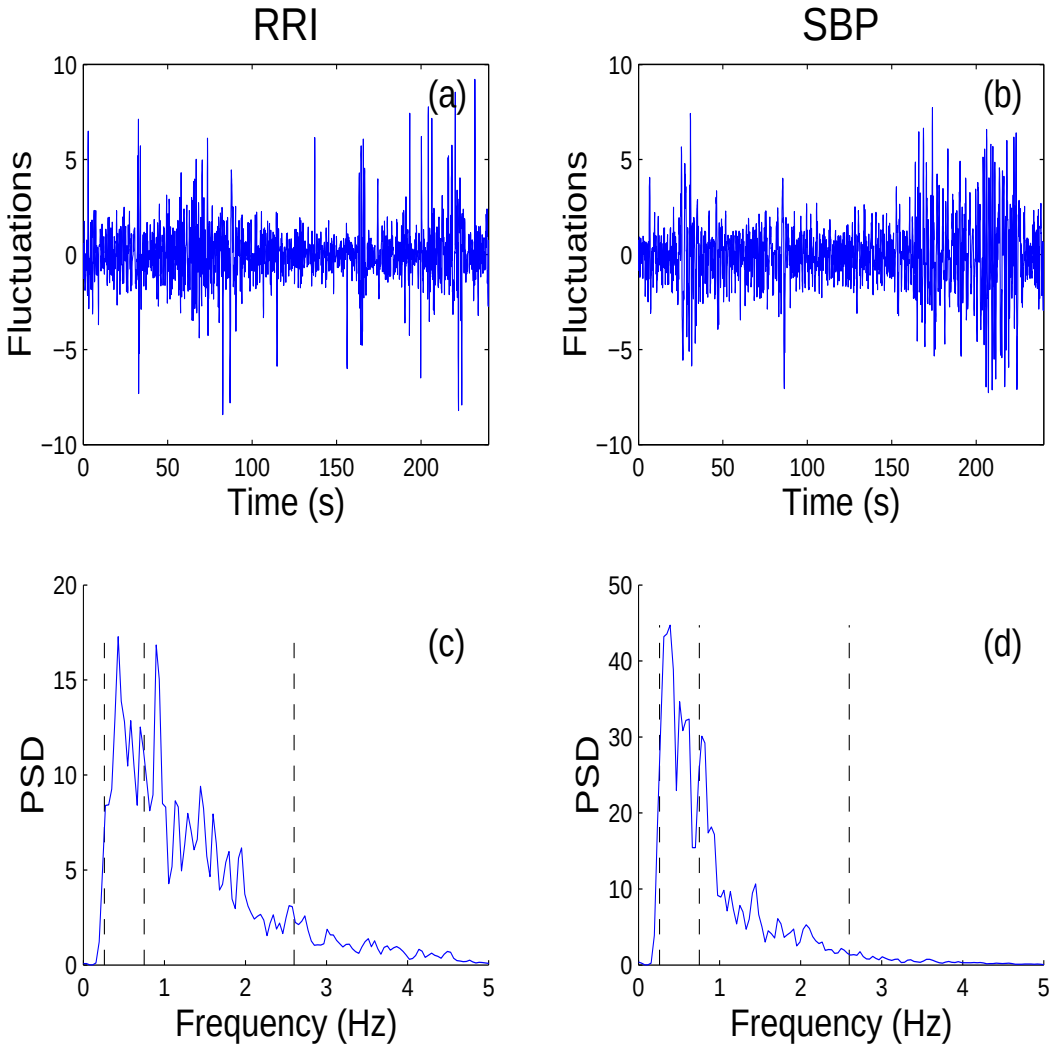

Figure 1: **Example 1.** For a chosen rat (Phentolamine Injection): left column, RR Intervals (RRI), right column, systolic blood pressure (SBP), top row, time series, bottom row, Power Spectral Densities estimates (in $10^3 ms^2/Hz$ for RRI and $10^3 mmHg^2/Hz$ for SBP), obtained from periodograms. The vertical dashed lines indicate the VLF, LF and HF rigid a priori frequency bands. Equivalent plots for each rat and each injection are available upon requests.

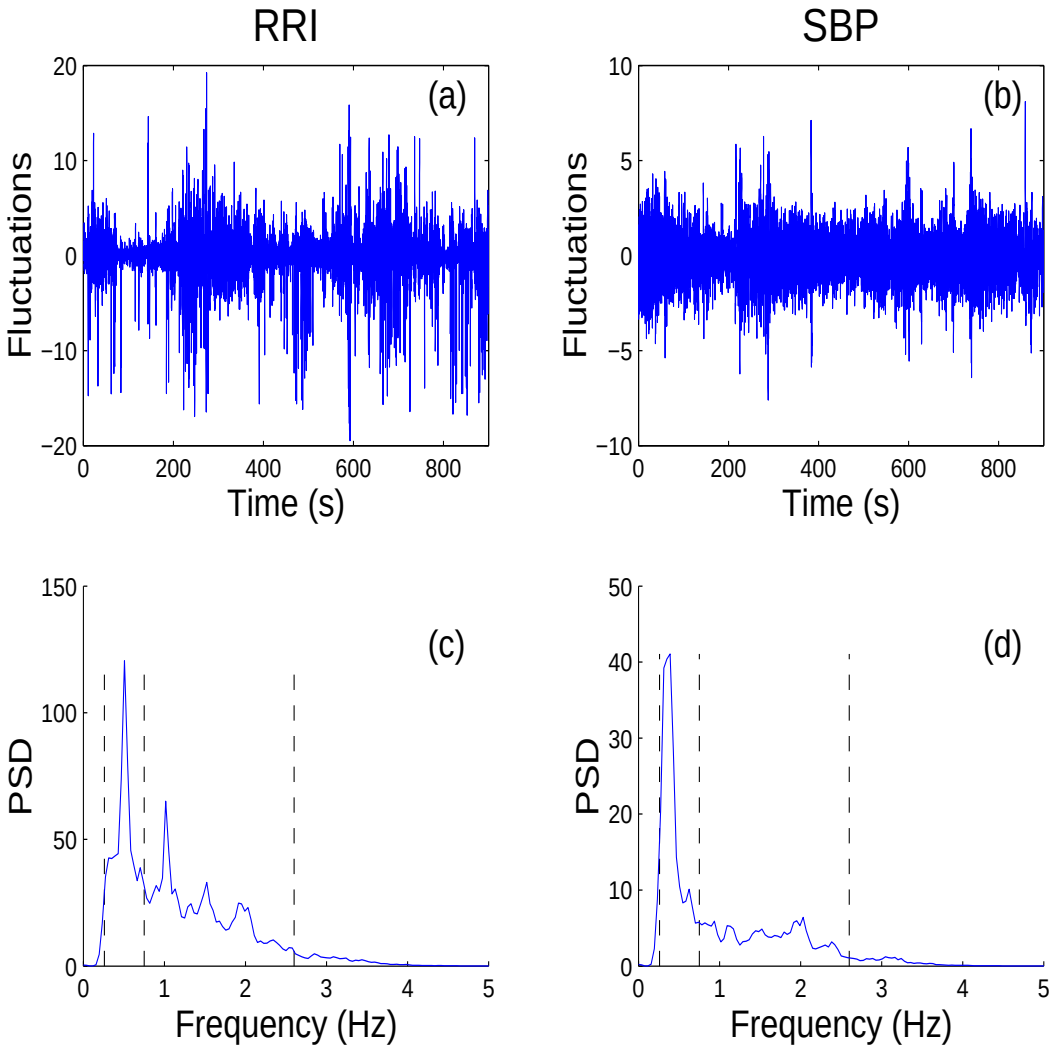

Figure 2: **Example 2.** For a chosen rat (no Injection). Legend as in Fig. 1.

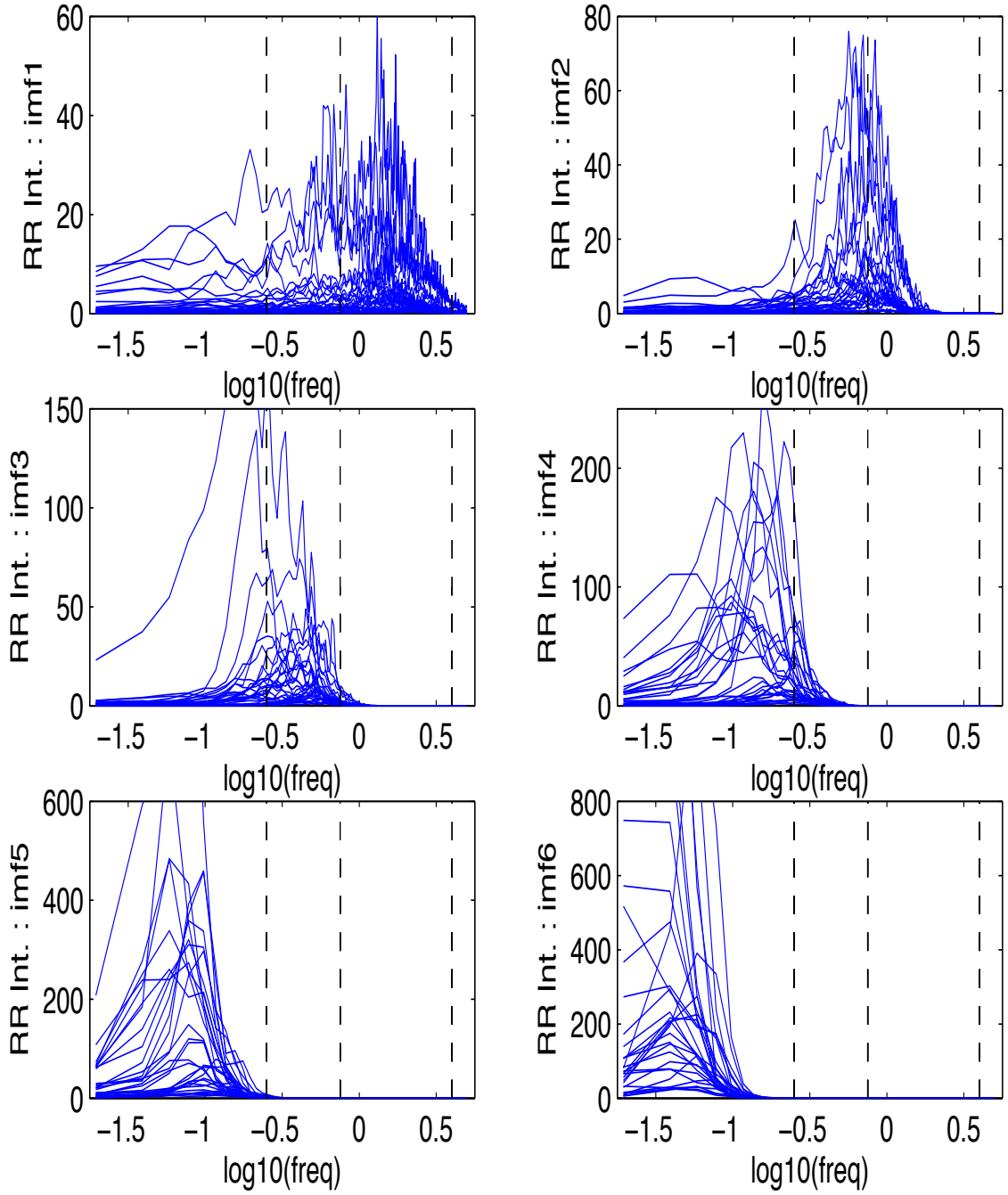

Figure 3: **RR Intervals IMFs for all subjects.** Superimposition of the 6 first IMFs for the RR Intervals signals of the 40 experiments (non normalized log-lin plots). The vertical dashed lines show the VLF, LF and HF rigid a priori frequency bands. This shows that IMF1 and IMF2 are mainly concentrated in the HF band while that IMF3 and IMF4 essentially correspond to the LF one. IMF5 and of higher order are clearly living in lower frequency ranges.

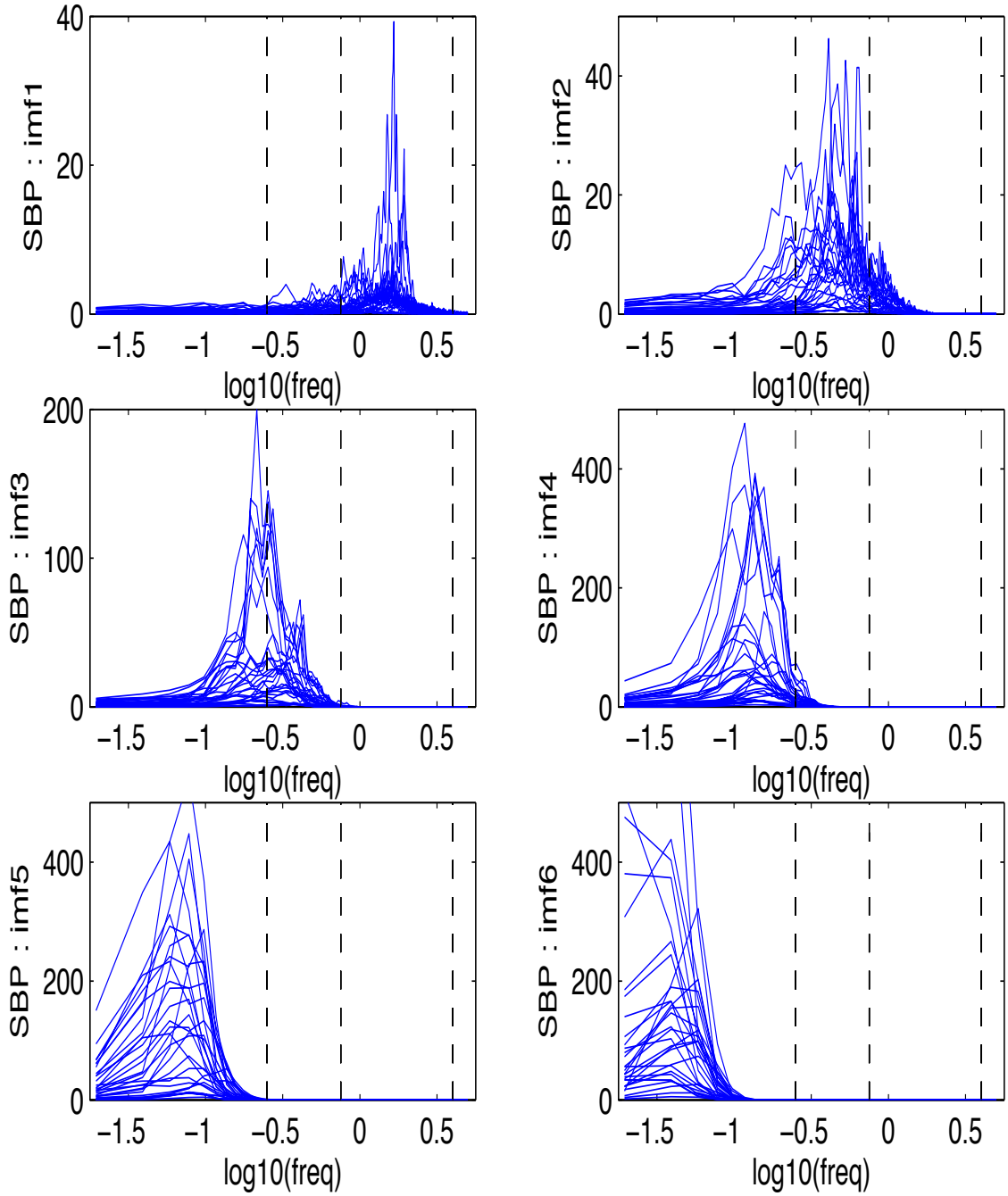

Figure 4: **Systolic blood pressure IMFs for all subjects.** Superimposition of the 6 first IMFs for the systolic blood pressure (SBP) signals of the 40 experiments (non normalized log-lin plots). This shows that IMF1 is mainly concentrated in the HF band while that IMF2 and IMF3 essentially correspond to the LF one. IMF4 and of higher order are clearly living in lower frequency ranges.

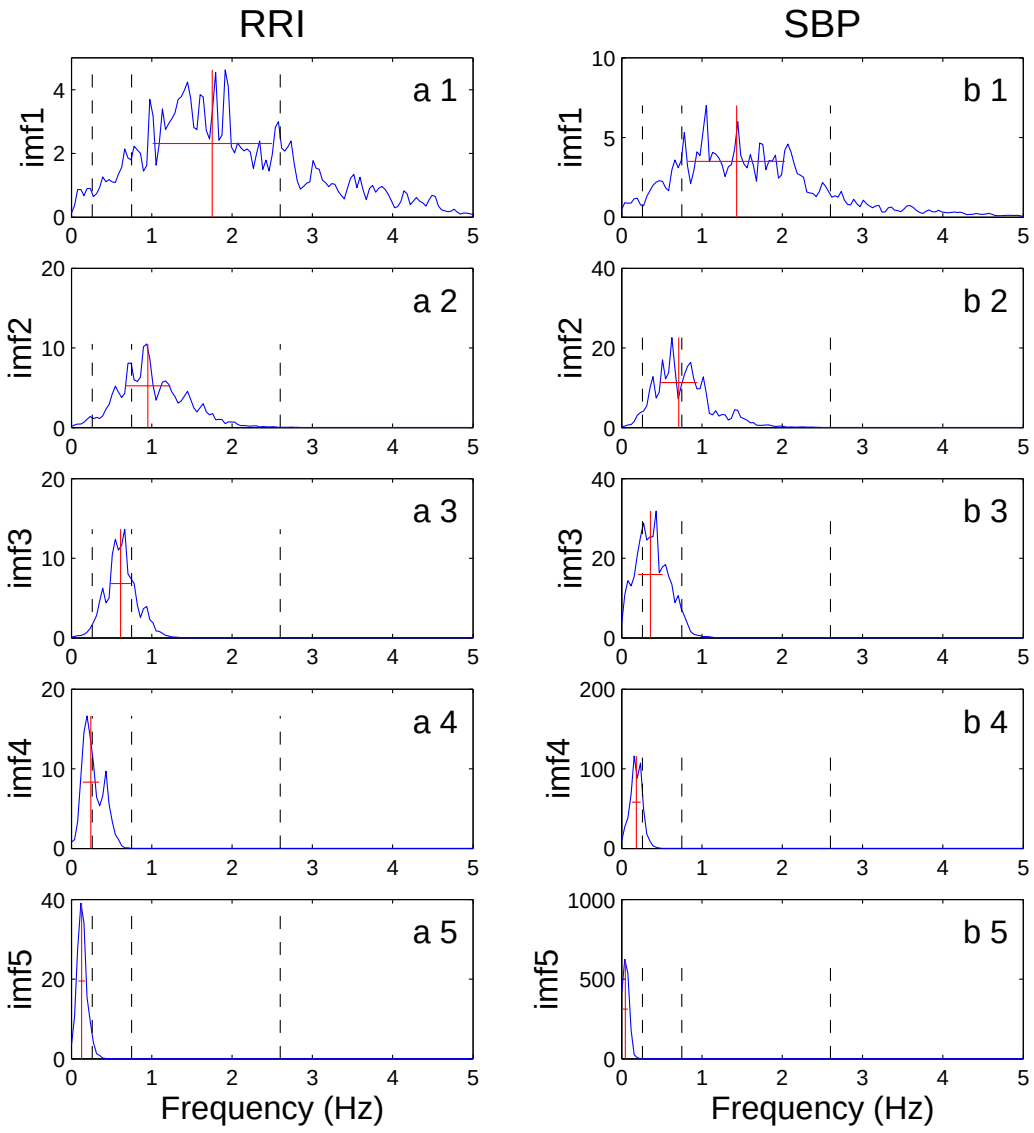

Figure 5: **IMFs for Example 1.** Spectral estimates for the five first IMFs for the RR Intervals (left column) and systolic blood pressure (right column) for the rat chosen as Example 1 in Fig. 1. Vertical dashed lines indicate the VLF, LF and HF rigid a priori frequency bands. The solid line crosses denote the central frequency plus and minus one standard bandwidth (cf. Section 3.3.2 for definition) for each IMF. These plots highlight on an example that, for RR Intervals, the spectral contents of IMF1 and IMF2 are mainly spread in the HF band while the spectral contents of IMF3 and IMF4 essentially live in the LF one and that, for systolic blood pressure, the spectral content of IMF1 is mainly spread in the HF band while the spectral contents of IMF2 and IMF3 essentially live in the LF one. Equivalent plots for each rat and each injection are available upon requests.

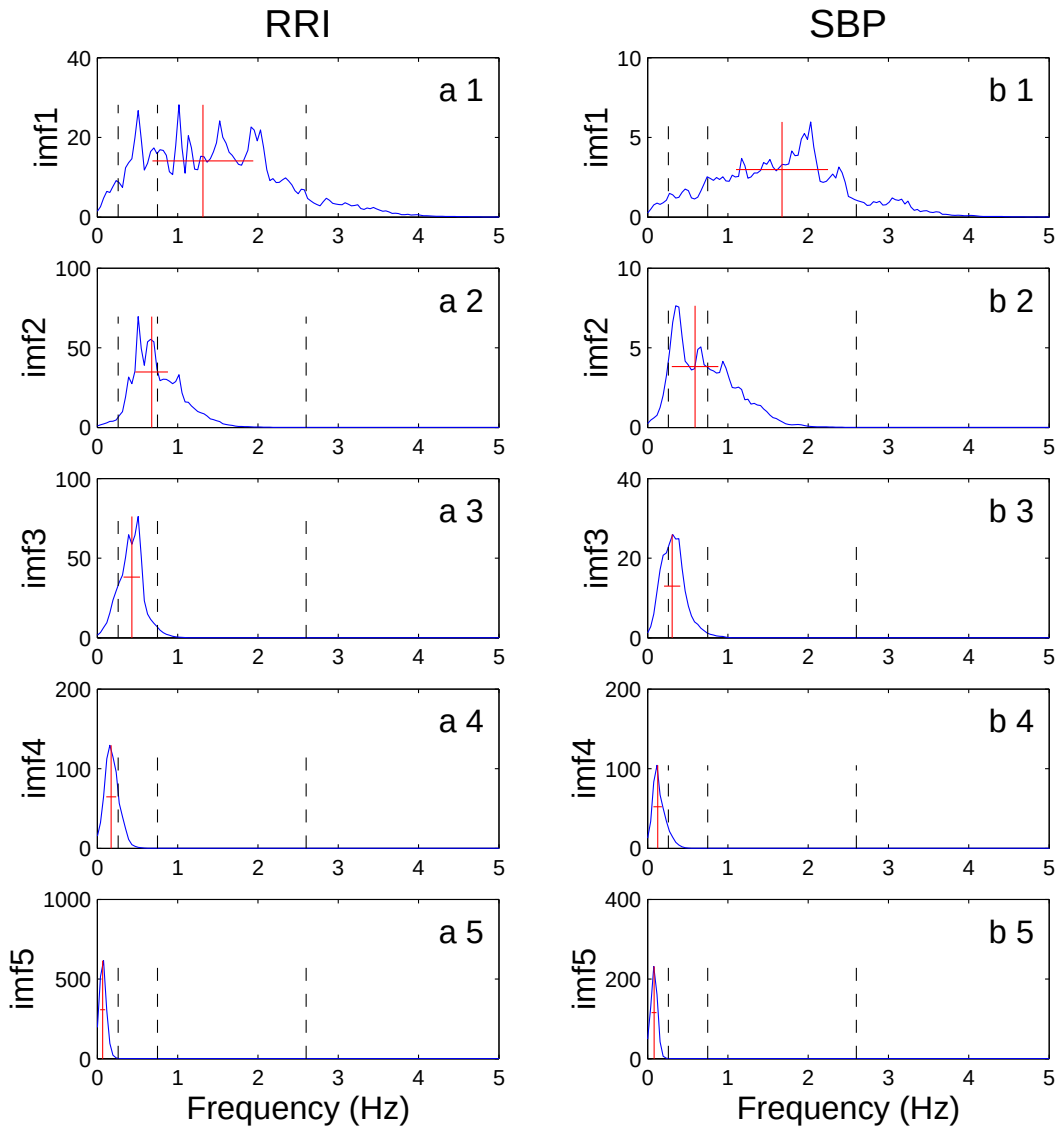

Figure 6: **IMFs for Example 2.** Legend as in Fig. 5. Compared to those in Fig. 5, these plots show that the central frequencies are mostly shifted towards low frequencies.

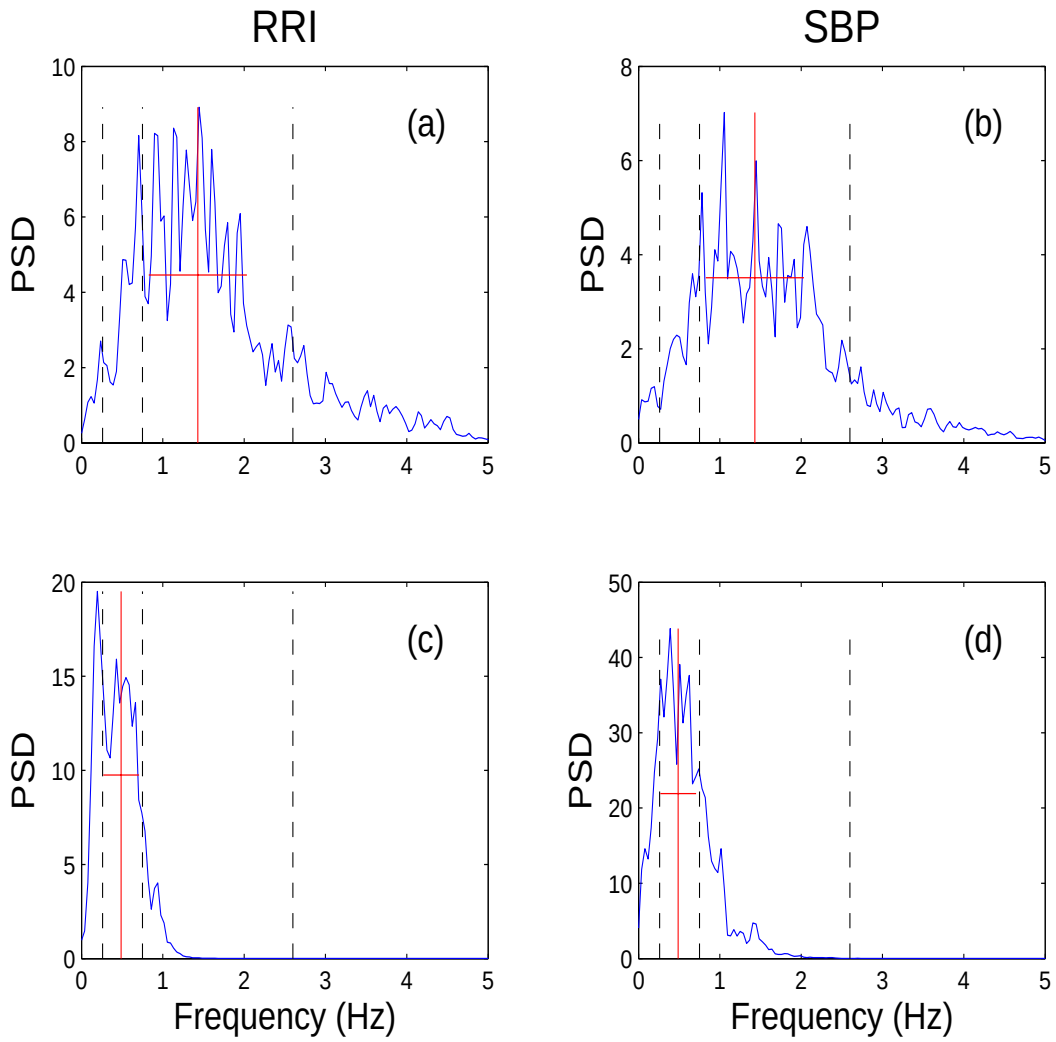

Figure 7: **EMD based LF and HF associations for Example 1.** Spectral estimates for the HF (top) and LF (bottom) EMD based contributions for the RR Intervals (left column) and systolic blood pressure (right column) for the rat chosen as Example 1 in Fig. 1. Vertical dashed lines indicate the VLF, LF and HF rigid a priori frequency bands. The solid line crosses denote the central frequencies plus and minus one standard bandwidth (computed from the SBP signal, cf. Section 3 for definition). These crosses delimitate the frequency bands over which the Alpha Gains are computed. On this example, one sees that the EMD based HF and LF decomposition spontaneously matches the HF/LF a priori and rigid frequency band one.

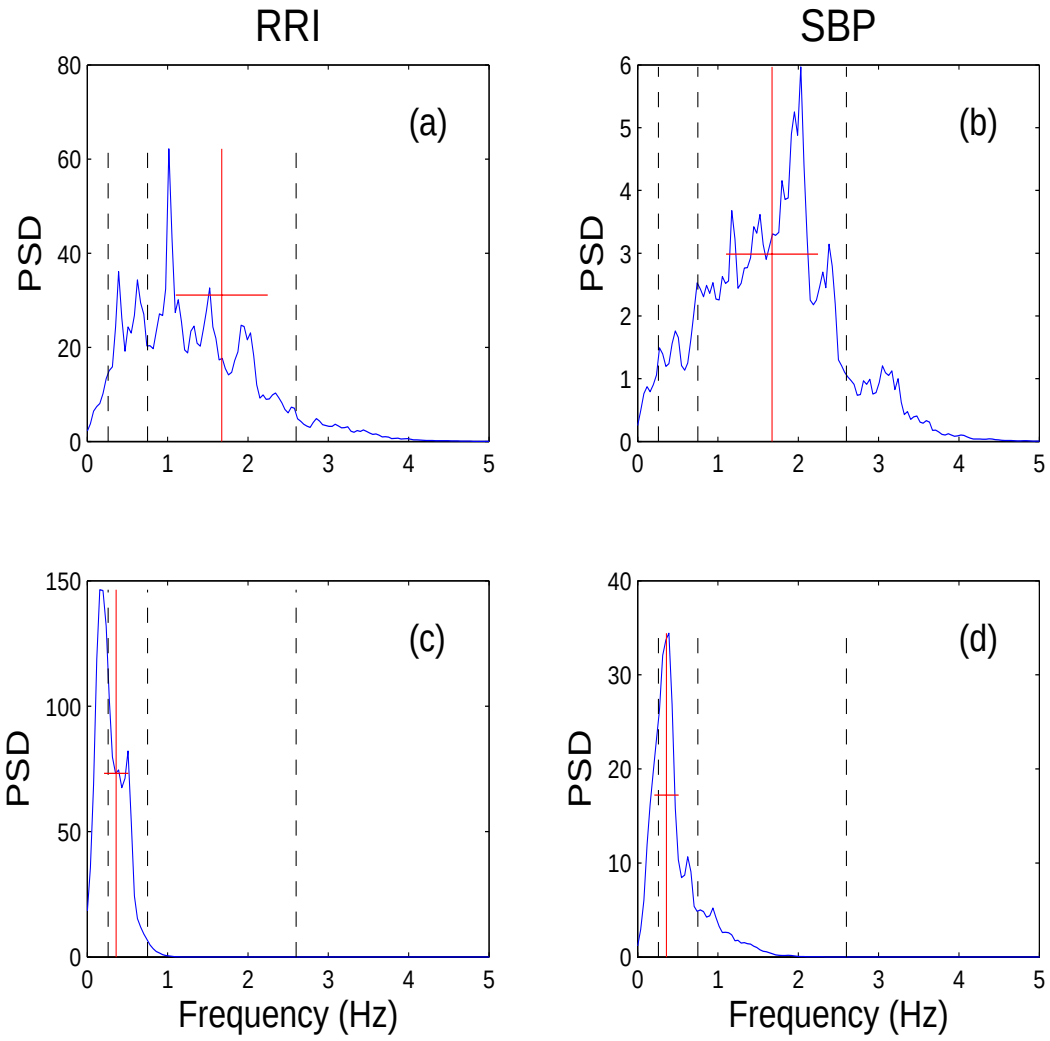

Figure 8: **EMD based LF and HF associations for Example 2.** Legend as in Fig. 7. Compared to those in Fig. 7, these plots indicate that the EMD based HF and LF separation may differ from the HF/LF a priori and rigid frequency band decomposition, here it is shifted towards low frequencies. This is where the EMD based non standard spectral analysis brings a significant contribution: it is signal adaptive so that it can spontaneously adjust to the natural shifts in the actual HF and LF frequency contents of the data.